

# Laboratory-scale Investigation of the Influence of Ageing on the Performance and Sensitivity of an Explosive Containing $\epsilon$ -CL-20

Jennifer L. Gottfried,<sup>\*,[a]</sup> Rose A. Pesce-Rodriguez,<sup>[a]</sup> Darcie Farrow,<sup>[b]</sup> and Jennifer Dellinger<sup>[b]</sup>

**Abstract:** The performance and sensitivity of aged composite explosives based on the epsilon polymorph of hexanitrohexaazaisowurtzitane ( $\epsilon$ -CL-20) have been evaluated with the laser-induced air shock from energetic materials (LASEM) technique using only milligram quantities of material. The LASEM results demonstrated reduced explosive performance (i.e., lower estimated detonation velocities) and higher sensitivity to ignition with increasing ageing. Chemical analysis of the explosive formulation subjected to

ambient and accelerated aging was conducted to help understand the LASEM results. The Fourier Transform Infrared (FTIR) spectra revealed no evidence for conversion to lower-energy polymorphs. Based on the desorption gas chromatography/mass spectrometry (D-GC/MS) results, the observed decrease in performance and increase in sensitivity for the explosive powder aged at 100 °C (relative to ambient and 70 °C aging) have been attributed to changes related to solvent inclusions in the molding powders.

**Keywords:** CL-20 • detonation performance • aged energetic materials • laser-induced plasma • laser-induced shock velocity • deflagration

## 1 Introduction

The sensitivity and stability of aged energetic materials is of key importance for the maintenance of military stockpiles. Direct measurement of the explosive performance (e.g., detonation velocity) and sensitivity (e.g., to friction, impact, electrostatic discharge) of a material requires at least tens of grams of material for multiple types of tests with significant safety hazards and costs. Laboratory-scale methods for characterizing energetic materials on the milligram scale are thus of substantial interest wherever energetic materials are produced or stored.


RSI-007 is a hexanitrohexaazaisowurtzitane (CL-20)-based molding powder (97.75 % explosive, 2.25 % proprietary binders). CL-20 was developed in 1987 at the Naval Air Weapons Station China Lake [1], and is currently the most powerful military explosive in use. There are five known polymorphs of CL-20 [2], although only the  $\alpha$ ,  $\beta$ ,  $\gamma$ , and  $\epsilon$  polymorphs exist at ambient conditions. The thermal stability of the polymorphs has been studied [3,4], and the  $\epsilon$  polymorph was found to be the most stable at room temperature. The  $\alpha$ ,  $\beta$ , and  $\epsilon$  polymorphs can be converted to the  $\gamma$  polymorph if heated to 155–198 °C [5]. The  $\epsilon$  polymorph has the highest density and the best explosive performance [6].

Here, we have investigated the degradation of aged composite energetic materials (RSI-007) using a non-detonative laboratory-scale technique requiring only tens of milligrams of material, the laser-induced air shock from energetic materials (LASEM) method. The LASEM method is based on the laser-induced shock wave velocity generated

when a nanosecond-pulsed laser is focused on a thin residue of energetic material [7,8]. The energetic material is ablated into the air above the sample surface, and a laser-induced plasma forms. The plasma, which lasts for tens of microseconds, is a high-temperature, highly ionized environment similar to the chemical reaction zone behind a detonation wave. The expansion of the laser-induced plasma into the air above the sample leads to the formation of the laser-induced shock wave. Both the energy from the laser [9,10] and the exothermic chemical reactions in the laser-induced plasma [7,11] contribute to the expansion of the shock wave. A strong linear correlation between the laser-induced shock wave from a laser-excited energetic material and the reported detonation velocities from large-scale testing has been previously observed [8]. This correlation has been used to estimate the detonation velocity of recently synthesized novel energetic materials [12,13] and composite energetic materials containing metal additives [14]. An-

[a] Dr. J. L. Gottfried, Dr. R. A. Pesce-Rodriguez  
Weapons and Materials Research Directorate  
US Army Research Laboratory  
Aberdeen Proving Ground, MD 21009  
\*e-mail: jennifer.l.gottfried.civ@mail.mil

[b] Dr. D. Farrow, Dr. J. Dellinger  
W78 Stockpile Systems/Energetics Characterization  
Sandia National Laboratories  
Albuquerque, NM 87185

 Supporting information for this article is available on the WWW under <https://doi.org/10.1002/prop.201800042>

alytical characterization of the baseline and aged RSI-007 samples was also performed to explain the LASEM results.

## 2 Experimental Section

### 2.1 Samples

Pure samples of  $\epsilon$ -CL-20 and  $\beta$ -CL-20 (with the latter aged under ambient conditions for more than 25 years) were obtained from storage magazines at the US Army Research Laboratory for comparison with the RSI-007 molding powders provided by Sandia National Laboratories. The  $\beta$ -CL-20 sample was used as provided for all experiments. Some of  $\epsilon$ -CL-20 sample was placed in differential scanning calorimetry (DSC) pans with a small amount of either ethyl acetate or chloroform ( $\text{CHCl}_3$ ); the solvents were evaporated under ambient conditions and Fourier transform infrared (FTIR) spectra were acquired of the  $\epsilon$ -CL-20 samples with adsorbed solvents.

The baseline RSI-007 (27 mg) had been stored under ambient conditions, while additional RSI-007 samples had been aged for 5 years at either 70 °C (44 mg) or 100 °C (33 mg). The RSI-007 powder was thermally aged (originally in 1 g quantities) under normal atmosphere. The free volume within the aging vessel exceeded 1 mL. All RSI-007 samples were used as provided with no further chemical treatment. Visually, the RSI-007 samples were more granular than the pure CL-20 (no particle size distribution information was available for any of the samples). The sample aged at 70 °C was visually similar to the baseline, although during weighing on a balance accurate to 1  $\mu\text{g}$ , slow mass loss typical of solvent evaporation was observed. The sample aged at 100 °C also appear to undergo solvent evaporation during weighing, and was slightly discolored (yellow) compared to the baseline powder.

### 2.2 LASEM

Two different sample preparation methods were compared for the LASEM analysis. Since pressed pellets of energetic material require significantly larger amounts of material (and preparation time), typically LASEM samples are prepared as thin residues pressed into double-sided tape affixed to a glass microscope slide [8]. Although other secondary military explosives are insensitive enough that the chemical reactions initiated by the focused 1064 nm laser pulse do not propagate beyond the focal volume of the laser, CL-20 residues have occasionally undergone flame spread reactions across the sample surface following laser excitation (see Fig. S1 from the Supporting Information for Ref. [15]). Because of the limited quantities of aged energetic material available for analysis, we first prepared the samples for LASEM analysis as individual residue piles (5 per microscope slide) with a slightly larger diameter (approx-

imately 1.5 mm) than the focused laser pulse. The average amount of material per pile (for the  $\epsilon$ -CL-20 and 3 RSI-007 samples) was  $754 \pm 156 \mu\text{g}$ . The goal was to avoid igniting the entire slide of material with one laser shot. A total of 15 laser shots for each of the 4 materials were acquired, and it was observed that all of the material in each pile either reacted or was ejected from the slide following each laser pulse. For comparison, thin residue samples were also prepared following the previously described method [8]. The average residue density for the 5 samples prepared this way (including  $\beta$ -CL-20) was  $13.8 \pm 2.8 \mu\text{g}/\text{mm}^2$ . A total of 20 laser shots per sample were obtained with this method, and no reaction propagation was observed for any of the samples.

The experimental setup has previously been described in detail [7,8,13,14]. Briefly, a 6-ns pulsed laser at 1064 nm (Quantel Brilliant b, 850 mJ) was focused just below the sample surface; the ablated material was vaporized and ionized, forming a high-temperature laser-induced plasma above the sample surface. The emission from the plasma and subsequent chemical reactions was recorded using a 100-ms gated spectrometer (Ocean Optics, USB4000, 200–890 nm) triggered by the Q-switch signal from the laser (i.e., zero time delay) and a time-resolved infrared-sensitive photoreceiver (New Focus Model 2053, 900–1700 nm). A Z-type schlieren imaging system illuminated with a 200 W Hg–Xe arc lamp was used to visualize the expansion of the laser-induced shock wave into the air above the sample. High-speed videos of the shock wave expansion were recorded with a Photron SA5 camera at 84,000 frames-per-second, 1.0  $\mu\text{s}$  exposure time,  $64 \times 648$  pixels image size. The characteristic laser-induced shock velocity in air for a sample under the specified experimental conditions was determined by finding the y-intercept of a polynomial fit to the velocity vs. time curve, and estimated detonation velocities were calculated using the previously determined calibration fit obtained under the same experimental conditions [8].

### 2.3 Analytical Characterization

Desorption and pyrolysis products were analyzed by means of a gas chromatography/mass spectrometry instrument with a desorption interface (D-GC/MS). Desorption was achieved via a CDS Analytical Model 2000 Pyroprobe® (coil type) connected through a heated interface chamber to the splitless injector of an Agilent (Santa Clara, CA) GC/MS system (Model 6890N GC and Model 5973N MSD). The GC column used was a HP-5 capillary column (0.25 mm  $\times$  30 m, 0.25- $\mu\text{m}$  film). The injector temperature was 200 °C; the Pyroprobe interface was set to a temperature of 175 °C. The GC oven temperature program was as follows: 100 °C isothermal for 1 min, 100–250 °C at 40 °C/min, and 250 °C isothermal for 1 min. The Pyroprobe was programmed to give a 20-s desorption pulse at either 175 or 250 °C at a heating

rate of 1,000 °C/s. The pulse temperature is based on calibration provided by the vendor and was not measured for this study. Samples (~1 mg) were held within the coil of the Pyroprobe by first placing them in a quartz tube containing a small plug of glass wool, and then inserting the entire tube into the coil. Selected ion chromatograms (SICs) were obtained via Hewlett Packard ChemStation software by extracting specified masses from the total ion chromatogram (TIC).

FTIR spectra of isolated particles were obtained using a Nicolet iS50 FTIR spectrometer interfaced to a Continuum IR microscope operating in reflectance mode and equipped with a ReFlacromat 15× objective. In order to get spectra that were not saturated, samples were gently spread in a thin layer on the substrate with the flat end of a spatula. For each spectrum, 128 scans were collected at a resolution of 4 cm<sup>-1</sup>. Spectral searches were performed using the Bio-Rad KnowItAll® Informatics System (Analytical Edition) software and database.

### 3 LASEM Results

#### 3.1 Emission Spectra

The emission spectra resulting from the pulsed laser excitation of the energetic materials provide information about the elemental content of the sample (including impurities) [16, 17], the chemical reactions in the laser-induced plasma [11, 13, 14, 18], and any combustion reactions that occur after the plasma is gone (millisecond timescale) [13–15]. Similar emission features were observed in the β-CL-20, ε-CL-20, RSI-007 baseline, and two aged RSI-007 samples (Figure 1); no emission features from non-organic impurities or the binder materials were detectable. Although most of the oxygen (O) and nitrogen (N) emission is due to air entrained in the laser-induced plasma, the β-CL-20 and RSI-007 sample aged at 100 °C have more O emission than the other samples. In addition, the ratio of the high-pressure di-

atomic carbon (C<sub>2</sub>) bands (formed through collisional excitation of lower vibrational state C<sub>2</sub> molecules) to the common C<sub>2</sub> Swan bands (e.g., at 516.5 nm) [C<sub>2</sub>\*/C<sub>2</sub>] is significantly higher for the CL-20-based energetic materials than for the inert blank tape, as previously observed for other explosives under development [13]. The calcium hydroxide (CaOH) band at 622 nm is also significantly higher for the energetic materials. CaOH is formed by the reaction of calcium (Ca) (common sample impurity) with O and hydrogen (H) after the laser-induced plasma is gone, and is indicative of the extended combustion reactions that occur on the millisecond timescale. The strong sodium (Na) and potassium (K) lines resulting from contamination (often from solvents used in the synthesis or purification steps) are also indications of extended combustion, since unlike C, H, N, or O they do not react to form molecular species during combustion and thus continue to emit for longer periods of time. For easier visualization of weaker emission features, Figure S1 in the Supporting Information shows the stacked spectra.

A comparison of the emission spectra for the samples prepared either as individual piles of material or as a thin residue is shown in Figure S2. Despite the fact that all the CL-20 in the individual piles appeared to react following laser excitation, the emission spectra show that more combustion occurred for the thin residue samples (indicated by the stronger CN, CaOH, Na, and K emission). Previous studies have shown that the material that is ejected off the sample slide by the laser-induced shock wave into the air heated by the plasma and the passage of the shock wave combusts on the millisecond timescale [7, 15]. This suggests that the material in the piles of CL-20 reacted on the microsecond timescale, which could affect the measured laser-induced shock wave velocities (since more material would lead to additional exothermic reactions in the plasma, increasing the plasma temperature and accelerating the shock wave).

#### 3.2 Laser-induced Deflagration

The time-resolved emission from the laser-induced deflagration of pure CL-20 (β- and ε-) and the RSI-007 samples are shown in Figure 2. The first sharp spike in emission is from the laser-induced plasma, while the millisecond-timescale emission is from combustion reactions that occur when the material surrounding the laser ablation region is ejected into the air by the laser-induced shock wave. A comparison of the β- and ε-CL-20 polymorphs shows significantly less combustion from the β-CL-20. The RSI-007 baseline, which contains 2.25% binder in addition to the CL-20, also has a much weaker deflagration intensity. In contrast, ageing of the RSI-007 at higher temperatures resulted in increased deflagration intensities, suggesting increased thermal sensitivity for the aged composite energetic materials.

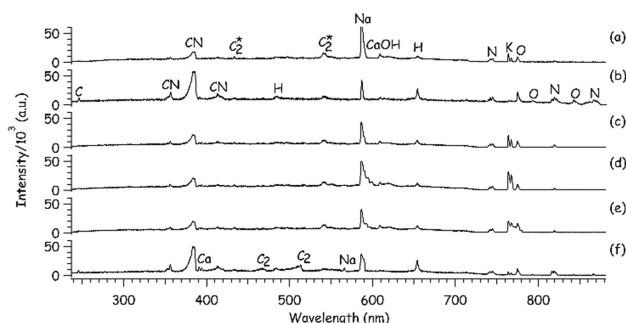


**Figure 1.** Emission spectra from the laser excitation of pure a) ε-CL-20 and b) β-CL-20, c) the RSI-007 baseline material aged at room temperature, the two RSI-007 samples aged at d) 70 or e) 100 °C, and f) the blank tape substrate.

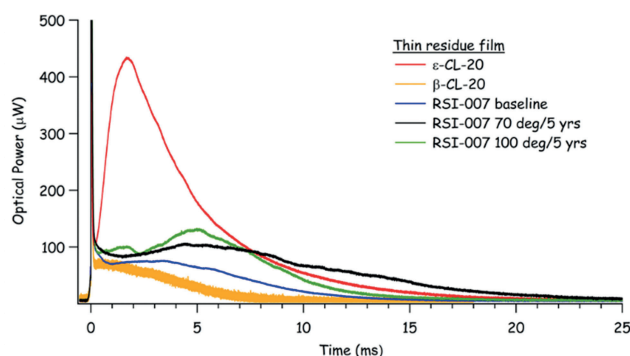


**Figure 2.** Time-resolved emission from the laser-induced deflagration of  $\beta$ - and  $\epsilon$ -CL-20, the RSI-007 baseline, and the two aged RSI-007 samples (prepared as a thin residue).

The effect of the sample preparation method on the laser-induced deflagration of  $\epsilon$ -CL-20 and RSI-007 aged at 100 °C is shown in Figure 3. As suggested by the emission spectra (Figure S2), the residue preparation method results in a stronger, longer lasting deflagration for the  $\epsilon$ -CL-20, since more material is available to be scattered into the air above the sample surface. While the pile of aged RSI-007 has a shorter time to peak deflagration and a more intense deflagration, the deflagration of the aged RSI-007 residue is delayed by about 5 milliseconds and lasts an order of magnitude longer. The difference in behavior based on sample preparation method observed for the RSI-007 sample compared to the pure CL-20 suggests that the presence of the binder delays the ignition of the scattered particles of CL-20 (which are more widely distributed as a result of the residue preparation method); similar delays to ignition were observed for all 3 RSI-007 samples, as shown in Figure 2.

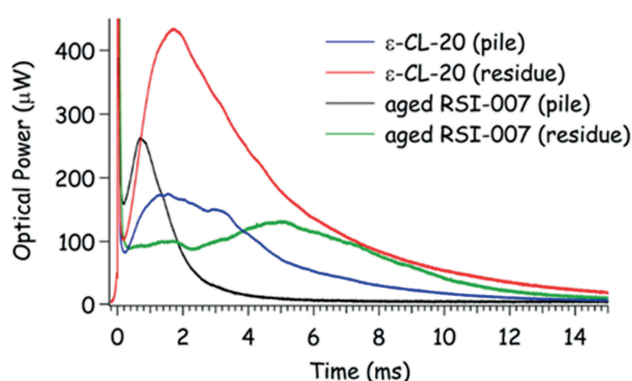


**Figure 3.** Effect of sample preparation methods on the time-resolved emission from the laser-induced deflagration of  $\epsilon$ -CL-20 and RSI-007 aged at 100 °C.

### 3.3 High-speed Videos

Figure 4 shows the first three frames from the high-speed videos of laser-excited  $\epsilon$ -CL-20 and the three RSI-007 samples (as well as the blank tape substrate for comparison). The first frame shows the laser-induced plasma emission, which we have previously demonstrated is generally more intense for nonenergetic materials [7]. We speculate that the laser ablated energetic materials more rapidly form products such as  $\text{CO}_2$  and  $\text{NO}_2$ , which do not have visible emission features; time-resolved emission experiments (on the microsecond-only timescale) are planned for future experiments to confirm this hypothesis. The aged RSI-007 samples have noticeably more significant plasma emission than the pure CL-20 or baseline RSI-007, suggesting that competing chemical reactions (with more visible emission) may be occurring – possibly due to a higher ratio of binder to CL-20.

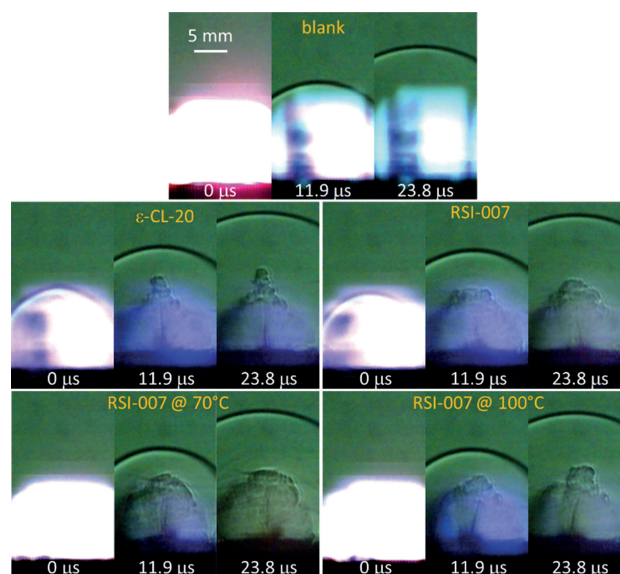


**Figure 4.** Snapshots from the high-speed videos of laser-excited  $\epsilon$ -CL-20, RSI-007 (baseline), and RSI-007 aged at either 70 or 100 °C.

### 3.4 Laser-induced Shock Velocities

When the characteristic laser-induced shock velocities were measured for the sample set prepared using piles of energetic material, significant overlap in the average shock velocities between all 3 RSI-007 samples was observed due to the unexpectedly large error bars (95% confidence intervals) for the aged samples. A closer look at the individual laser shots for the aged RSI-007 samples revealed that unusually high laser-induced shock velocities (exceeding that of pure CL-20) were measured for some laser shots. These results suggested that at least some of the material in the



sample pile outside the laser focus was reacting quickly enough to influence the laser-induced shock wave. Figure S3 demonstrates the effect of sample preparation on the measured laser-induced shock velocities. For the pure  $\epsilon$ -CL-20, there is no statistical difference between the average shock velocities for the pile vs. residue sample preparation methods. While the difference between the RSI-007 baseline shock velocities are not statistically significant either (at the 5% level), the shock velocities for the aged RSI-007 sample are significantly higher when the samples were prepared as individual piles of material. These results confirm the increased sensitivity for the aged samples suggested by the laser-induced deflagration behavior (Figure 2), and demonstrated that the propagation of the laser-initiated reaction beyond the laser focus due to the sensitivity of the material can increase the measured laser-induced shock velocity. Since no evidence for reaction propagation was observed for the thin residue samples, only the shock velocities measured from residue samples were used to compare the detonation performance of the composite energetic materials.

The characteristic shock velocities obtained using the thin residue sample preparation method for the pure CL-20 samples and the 3 RSI-007 samples (along with the explosive trinitrotoluene [TNT] for comparison) are shown in Figure 5. The  $\beta$ -CL-20 (density = 1.985 g/cm<sup>3</sup>) [5] has significantly less energy release than the  $\epsilon$ -CL-20 (density = 2.044 g/cm<sup>3</sup>). While the  $\beta$  polymorph is predicted to have a lower detonation velocity than the  $\epsilon$  polymorph [6], our particular  $\beta$ -CL-20 sample had been stored in a magazine for more than 25 years and may have undergone other, as yet unidentified, changes that adversely affected the performance (no studies of long-term ageing of  $\beta$ -CL-20 have been reported). No other polymorphs were readily available for comparison. In addition, Figure 5 shows that the baseline RSI-007 has lower energy release than pure  $\epsilon$ -CL-20. Not only does the binder have a desensitizing effect on CL-20, it also reduces the detonation performance (as previously predicted [19]). Ageing of the RSI-007 sample also resulted in decreased energy release, with the sample aged at 100 °C

producing the lowest measured shock velocity of the 3 RSI-007 materials.

In order to confirm that differences observed in laser-induced shock velocities for the RSI-007 samples are statistically significant, a multiple comparison of means test (based on Fisher's least significant difference procedure) was performed using Matlab. As shown in Figure S4, at the 5% significance level,  $\epsilon$ -CL-20 and the RSI-007 baseline have different shock velocities. In addition, the aged RSI-007 samples (70 and 100 °C) are statistically different from each other and the RSI-007 baseline. These results confirm that LASEM is sensitive to the performance degradation of aged energetic materials (and the presence of nonenergetic binder materials).

The estimated detonation properties (at the theoretical maximum density [TMD]) of both CL-20 polymorphs and all 3 RSI-007 samples were calculated based on the previously determined correlation fits between the laser-induced shock velocities and the measured detonation velocities and pressures from large-scale detonation testing [8]. As shown in Table 1, the LASEM results predict a 5.7% decrease in detonation velocity for the RSI-007 sample aged at 70 °C compared to the baseline RSI-007 and a 12.5% decrease in detonation velocity for the RSI-007 sample aged at 100 °C.

**Table 1.** Estimated detonation properties of  $\beta$ - and  $\epsilon$ -CL-20 and 3 RSI-007 samples.

Sample	Laser-induced shock velocity (m/s)	Estimated detonation velocity @ TMD (km/s)	Estimated detonation pressure @ TMD (GPa)
$\epsilon$ -CL-20	835.41 ± 9.52	9.56 ± 0.24	42.86 ± 2.08
RSI-007 baseline	816.08 ± 9.92	9.08 ± 0.25	38.65 ± 2.16
RSI-007 (aged @ 70 °C)	795.10 ± 11.56	8.56 ± 0.29	34.07 ± 2.52
RSI-007 (aged @ 100 °C)	769.84 ± 11.90	7.94 ± 0.29	28.56 ± 2.60
$\beta$ -CL-20	721.67 ± 16.10	6.75 ± 0.40	18.06 ± 3.51

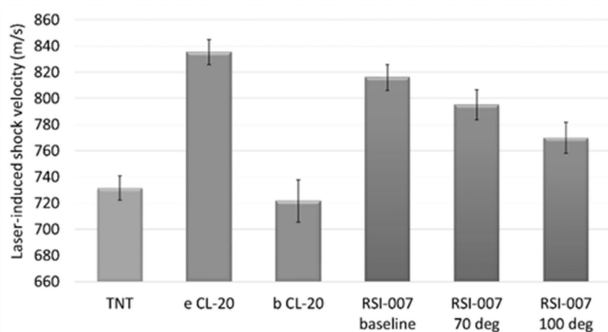


**Figure 5.** Laser-induced shock velocities measured from the laser excitation of thin residues of pure TNT,  $\beta$ -CL-20, and  $\epsilon$ -CL-20 explosives, as well as the RSI-007 baseline and aged RSI-007 composite energetic materials.

## 4 Analytical Characterization Results

### 4.1 Reflectance FTIR-microscopic Analysis

Representative FTIR spectra are given in Figure 6 and show that for both baseline and 100 °C-aged samples, there were two types of observed spectra. The traces in Figure 6 without an asterisk are as expected for  $\epsilon$ -CL-20 spectra [20, 21]. While powder yielding the anomalous asterisked traces was found for both ambient and 100 °C-aged samples, they were distinctly more prevalent in the baseline sample. The traces with an asterisk are very similar to spectra of  $\epsilon$ -CL-20 with respect to both wavenumber and intensity in the 1200–800 and 3080–3000 cm<sup>−1</sup> regions, but differ in relative

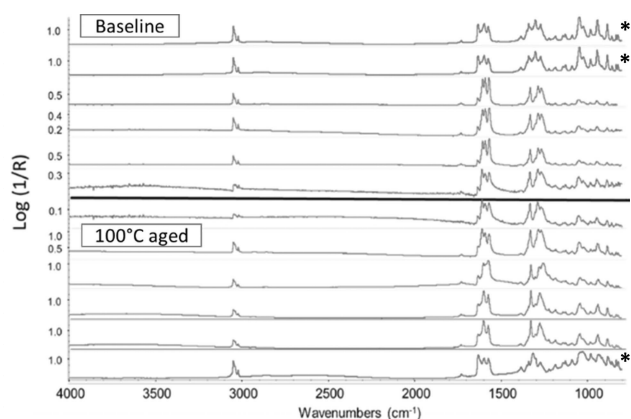


**Figure 6.** FTIR-microscope reflectance spectra of baseline (top 6) and 100 °C aged (bottom 6) RSI-007 samples. Non-asterisked traces are consistent with  $\epsilon$ -CL-20. Asterisked traces are generally consistent with  $\epsilon$ -CL-20 but have several anomalous peaks.

intensity in the 1700–1200  $\text{cm}^{-1}$  region. While the exact reason for this difference was not immediately clear, it was concluded that it is not the result of the presence of another CL-20 polymorph. The failure to convert to the gamma polymorph on 100 °C aging appears to be inconsistent with results reported by Foltz et al. [3] which suggest a thermodynamic transition temperature of approximately 64 °C for epsilon to gamma. However, it must be noted that this transition was observed by Foltz et al. only when solvents were used to “facilitate equilibrium.” Results for thermal treatment of dry  $\epsilon$ -CL-20 indicated that the transition to gamma is rate dependent [4], and that even at the slowest rate investigated (0.5 °C/min) transition doesn’t occur below 150 °C.

The FTIR-microscopic analysis of the 25-year old Class 5  $\beta$ -CL-20 sample was consistent with published spectra of  $\beta$ -CL-20 (green traces, Figure S5). Like with the RSI-007 samples, some of the spectra (red traces, Figure S5) contained anomalous peaks, albeit not the same ones observed for some RSI-007 particles. It appears that all the particles of  $\beta$ -CL-20 with the anomalous spectra have a relatively high level of  $\text{CHCl}_3$  and ethyl acetate. Both solvents are commonly used in the recrystallization of CL-20. Ethyl acetate is used to dissolve the material, while  $\text{CHCl}_3$  is an anti-solvent that is used to rapidly precipitate (“crash out”) crystals. In this process, the two miscible solvents are trapped in inclusions within the crystalline CL-20. It is also likely that a very low level, perhaps a monolayer, of ethyl acetate is also present on the exterior of CL-20 particles. This hypothesis is based on previous analysis of cyclotrimethylenetrinitramine (RDX) in Composition-A3 by our group [22] as well as of neat RDX by Batten [23]. Both analyses resulted in the conclusion that RDX can retain a very small level of solvent even when heated up to 160 °C under vacuum. This “tenaciously held” solvent (as described by Batten) was proposed by us to be surface-sorbed, possibly as a mono-layer. In the case of the

RSI-007 baseline sample, it is proposed that CL-20 has both included ethyl acetate and  $\text{CHCl}_3$ , as well as adsorbed ethyl acetate. As an anti-solvent for CL-20, it was assumed that  $\text{CHCl}_3$  would not surface-sorb to a significant extent, but the possibility was not completely ruled out.

It is proposed that the anomalous FTIR peaks in Figure S5 are the result of the interaction of  $\beta$ -CL-20 with included residual solvent. This would suggest that residual solvent is not distributed uniformly among all particles, and also suggests that the anomalous peaks for  $\epsilon$ -CL-20 in Figure 6 might also result from interaction with included solvent. Given that all particles examined in this study are ultrafine, it is reasonable to expect that FTIR radiation is able to easily penetrate all particles, and is therefore also subject to absorption by included solvent. It is also reasonable to expect that included ethyl acetate interacts with and partially solvates  $\epsilon$ -CL-20, as was proposed for  $\beta$ -CL-20. This hypothesis was confirmed with the spectra presented in Figure 7, which shows  $\epsilon$ -CL-20, as received (top trace) and with adsorbed  $\text{CHCl}_3$  (2nd trace) or ethyl acetate (3rd trace), along with a spectrum of anomalous particles from the 100 °C-aged RSI-007 sample (bottom trace). Precipitation of  $\epsilon$ -CL-20 from ethyl acetate results in  $\beta$ -CL-20 crystals; peaks consistent with  $\beta$ -CL-20 are present in the FTIR spectrum of  $\epsilon$ -CL-20 with adsorbed ethyl acetate in the region of 1200–600  $\text{cm}^{-1}$ . Peak shifts resulting from interaction with included solvents are observed in a very small fraction of particles of the 100 °C-aged sample, presumably because most inclusions had erupted during aging. More particles showing evidence of solvent interaction were observed for the ambient-aged sample since most inclusions were still intact.

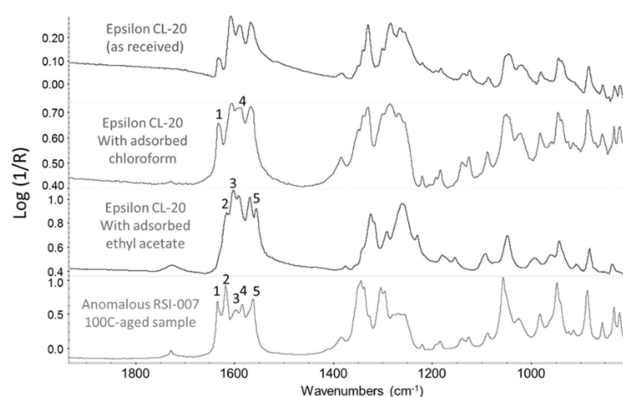


**Figure 7.** FTIR of  $\epsilon$ -CL-20 as-received and with adsorbed chloroform and ethyl acetate, and a representative spectrum of anomalous particles from the 100 °C-aged RSI-007 sample.

#### 4.2 D-GC/MS

The TICs of the baseline RSI-007 for two sequential desorption pulses (the first at 175 °C and the second at 250 °C)

are shown in Figure 8. Analysis of the D-GC/MS chromatograms revealed the presence of peaks due to the binders and binder additives at 6.7 min (top) and 8.7 min (bottom); based on their relative quantities in the 3 RSI-007 samples, these results were determined not to be relevant to the decreased performance and increased sensitivity observed for the aged RSI-007 samples. The large peak near 1.8 min in Figure 8 (bottom) results from CL-20 decomposition products; all are “permanent gas” products (i.e.,  $\text{CO}_2$ ,  $\text{N}_2$ ,  $\text{NO}$ ,  $\text{NO}_2$ ,  $\text{N}_2\text{O}$ ,  $\text{HCN}$ ,  $\text{HNCO}$ , etc.). The absence of larger CL-20 decomposition products suggests complete decomposition with no secondary reaction products.

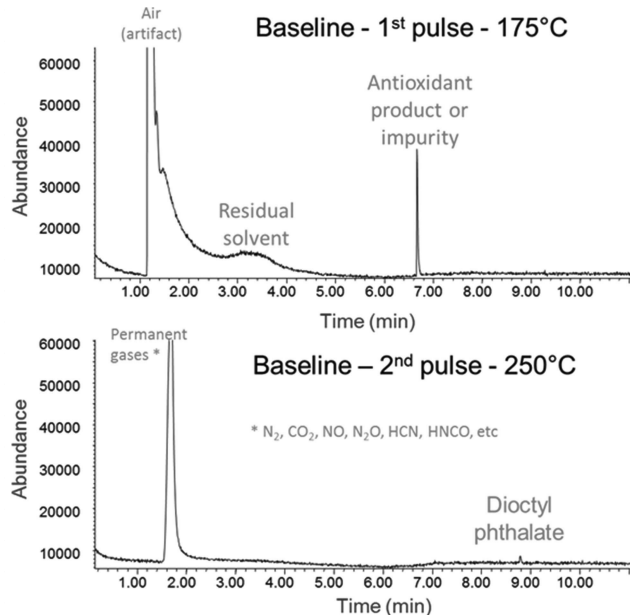


**Figure 8.** TICs of the baseline RSI-007 sample pulsed at 175 °C (top) and 250 °C (bottom).

The assignment of the broad peak centered near 3.4 min in Figure 8 (top) confirms the presence of  $\text{CHCl}_3$  and ethyl acetate, as indicated by the FTIR spectra analysis. The mass spectra of the peaks observed in the chromatograms of relatively small (~1 mg) and large (~2 mg) samples of the baseline RSI-007 sample are given in Figure S6. As shown in the SICs for the analysis of a large sample of neat  $\beta$ -CL-20 (Figure S7) there are two peaks that elute between 1.5–3.5 min. The mass spectra for each of the peaks as well as their spectral search matches are given in Figure 9, and confirm the presence of the residual solvents in the baseline RSI-007 (Figure S6; top of Figure 8).

The TICs for the 100 °C-aged RSI-007 sample when pulsed at 175 and 250 °C are shown in Figure S8. The 175 °C chromatogram showed neither included solvent nor antioxidant product, but does have a peak for a fluorescent whitening agent (FWA), i.e. 2,2'-(2,5-thiophenediyl)bis[5-(1,1-dimethylethyl) benzoxazole, which is also known as

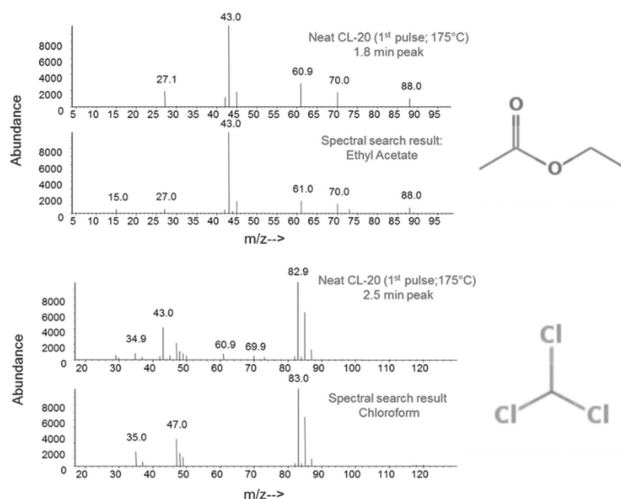


**Figure 9.** Mass spectra and search matches for 1.8 (ethyl acetate) and 2.5 min (chloroform) peaks in Figure S6; they also apply to the 3.4 min peak in Figure 8 (top), as shown in Figure S6.

Uvitex OB. The mass spectrum of the 5.9 min peak and Uvitex OB library spectrum are given in Figure S9. The FWA is likely present as an additive in one of the binders.

As noted above, when relatively small samples of RSI-007 are pulsed at 250 °C, CL-20 decomposition is very efficient and produces only permanent gas products. When larger samples are pyrolyzed at the same temperature, less efficient decomposition and secondary reactions occur, resulting in larger products. Figure S10 gives TICs for the baseline and 100 °C-aged samples pulsed at 250 °C; Figure S11 gives several SICs for the same samples. While permanent gas products are still observed, triazine and a number of larger (unidentified) nitrogen-containing cyclic products are also produced. No significant differences in the TICs or SICs for the baseline and aged samples pulsed at 250 °C were observed. It is noted that while a product with  $m/z=43$  is observed in the SICs, it is assigned to  $\text{HNCO}$ , and is not related to the  $\text{CH}_3\text{CO}$  radical with the same  $m/z$  value that was observed in the mass spectrum of ethyl acetate.

A comparison of SICs for all three RSI-007 samples at both 175 and 250 °C pulse temperatures are given in Figure 10. From the 175 °C chromatograms it is observed that aging at 70 °C was insufficient to remove solvent from inclusions, and that even when aged at 100 °C, some surface-sorbed or included solvent is still present. It is also observed that the CL-20 in 70 and 100 °C aged samples seems to decompose at a slightly greater extent than in the baseline sample, albeit at a very low level. When the same samples are pulsed for a second time at 250 °C, it appears that only the 70 °C aged sample shows an appreciable level of solvent evolution as evidenced by the blue  $m/z=43$  trace, but that is not the case. From the relatively elevated  $m/z=30$  ( $\text{NO}$ ) trace it may be concluded that CL-20 is decomposing and that the  $m/z=43$  trace should be assigned not to ethyl acetate, but to  $\text{HNCO}$ . There is no evidence of decom-

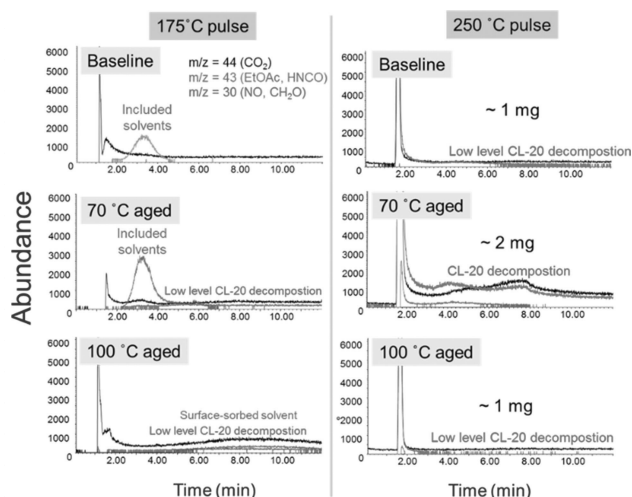


**Figure 10.** SICs for baseline (top), 70 °C aged (middle) and 100 °C aged (bottom) RSI-007 samples pulsed at 175 °C (left) and 250 °C (right).

position of the binders themselves in any of the chromatograms.

## 5 Discussion

Analysis of the three RSI-007 samples by LASEM led to two conclusions, i.e., that the 100 °C-aged sample appears to be more sensitive than the ambient or 70 °C-aged samples, and that the laser-induced shock velocity (i.e., microsecond-timescale energy release) was such that baseline > 70 °C-aged > 100 °C-aged. At this time, it is impossible to conclusively ascribe those differences in LASEM behavior to compositional differences, but we will offer several possible scenarios related to solvent inclusions that may explain the observed behavior.

From D-GC/MS analysis it was found that the baseline and 70 °C-aged samples have significantly more ethyl acetate and  $\text{CHCl}_3$  than does the 100 °C-aged sample, presumably because accelerated ageing at the higher temperature drove off most of the included solvent. In a previous analysis of RDX recrystallized from acetone [22] it was observed that heating RDX with solvent inclusions at 175 °C resulted in gentle “eruptions” of inclusions and concomitant crazing of the crystals. If the same phenomenon resulted for CL-20 in aged RSI-007, we should expect similar damage for CL-20 crystals, perhaps resulting in the greater sensitivity for the 100 °C-aged samples observed in LASEM tests. The effect of such mechanical damage on the laser-induced shock velocity is not clear at this time, but if solvent eruptions affected binder-filler interactions, then perhaps performance might be affected. A recent paper by Basset et al. [24] discussed the importance of “micropores” in energetic materials with respect to hotspot formation and shock initiation. The au-

thors discuss filling pores with various gases, but never mention the word “solvent” in their paper, so it is likely that they did not perform an analysis such as that presented herein. It is impossible to tell if their samples were solvent-free. In any case, their findings indicate the importance of “pores” or gas inclusions on sensitivity to shock initiation and hot spot formation. This supports the hypothesis that increased porosity from eruptions of inclusions in the 100 °C-aged sample could have resulted in increased sensitivity relative to unaged molding powder with intact solvent-filled inclusions.

Another possible scenario to explain LASEM results is related to the tendency of included ethyl acetate to dissolve CL-20, resulting in tiny pockets of ethyl acetate saturated with CL-20. The solubility of CL-20 in ethyl acetate is quite high, i.e., 406 mg/mL at 25 °C (p. 82 in Ref. [25]), and presumably considerably higher at 100 °C. Dissolved CL-20 will be rapidly lost along with included solvents when they first expand, then “erupt” from the inclusion, and finally are removed from the molding powder when entrained with evaporating solvent. The consequence is that formerly “energetic” inclusions that contained ethyl acetate saturated with CL-20 are converted to air-filled non-energetic inclusions, leaving a particle that is both slightly depleted in CL-20 and more sensitive because of the possibility of adiabatic compression of the air filling, resulting in hot spots. One would expect the amount of CL-20 lost from eruption of inclusions to be very small, but the LASEM data itself suggests that a subtle difference might be all that is needed to explain the observed results. This proposed scenario is consistent with both D-GC/MS and FTIR-microscope results.

It should be noted that loss of CL-20 from solvent eruptions will be more important for a molding powder than for a consolidated charge. In the former case, diffusion and evaporation of both solvent and dissolved CL-20 can take place easily and quickly; in the latter case diffusion and evaporation of dissolved CL-20 could occur only from exposed surfaces of the consolidated charge. Eruptions of inclusions within the charge would release solvent that could diffuse to exposed surfaces; dissolved CL-20 would also slowly diffuse to the exposed surface, but would then be more likely to crystallize (possibly resulting in a “bloom”) at that surface. Such a phenomenon has been observed for an RDX-filled triple-base propellant (“JAX”) on aging [26].

Another possible explanation for the lower laser-induced shock velocities of aged RSI-007 powders relative to unaged powder is sublimation of CL-20 during aging. Boddu [27] predicted vapor pressure for CL-20 at 100 °C to be 5 orders of magnitude higher than at 25 °C (log VP = −14.1 torr at 25 °C and −9.15 at 100 °C). Pesce-Rodriguez and Klier [28] predicted similar values (−12.5 torr and −7.2 torr, respectively, at 25 and 100 °C). While sublimation of CL-20 from a pressed charge would be expected to be small, non-negligible loss from a loose molding powder would be expected – resulting in a higher relative amount of binder to



CL-20. LASEM results have proven to be sensitive to binder concentrations of several percent (e.g., CL-20 vs. RSI-007 in this work, HMX vs. PBXN-5 or PBXN-9 [8], RDX vs. Composition-A3 [8]). This hypothesis was discounted based on unpublished results for quantitative analysis of CL-20 in ambient and 100 °C-aged samples via ultra-performance liquid chromatography (UPLC) performed by Sandia National Laboratories.

Overall, it is concluded that the most important difference found for the three RSI-007 samples is the level of included solvent. As porosity has historically been linked to hot spot formation, and as there has been a historical lack of characterization of what and how much material is inside pores or inclusions in energetic crystals, it may be time for more focused attention to this potentially important characteristic of energetic crystals, especially in light of the neglected fact that included solvents will dissolve energetic material from the walls of the inclusion and could potentially play an as yet unidentified role in the initiation or propagation process. D-GC/MS is exquisitely well-suited to such characterization and would be well paired with any investigation of performance of any kind.

## 6 Conclusions

We have demonstrated that LASEM can be used to compare the sensitivity and estimate the decrease in detonation performance for aged energetic materials using only minimal quantities of each sample (less than 20 mg). Both the emission spectra and the time-resolved emission demonstrated the increased sensitivity of the aged RSI-007 samples, resulting in increased combustion reactions on the millisecond timescale. This increased sensitivity also necessitated using a sample preparation method that avoided propagation of the laser-initiated reaction to the surrounding material. The measured laser-induced shock velocities for each of the pure CL-20 and RSI-007 samples were shown to be statistically different at the 5% significance level. The RSI-007 composite energetic material has 2.25% binders, which was enough to result in a slightly lower estimated detonation performance compared to pure  $\epsilon$ -CL-20. The estimated detonation performance of the RSI-007 sample aged at 100 °C was shown to be the lowest of the 3 composite energetic material samples, and the baseline RSI-007 sample aged at room temperature had the best estimated detonation performance (with the sample aged at 70 °C in between the other two). We also demonstrated differences in estimated performance for two CL-20 polymorphs ( $\beta$  and  $\epsilon$ ).

The remaining material from this study was used to perform a comprehensive analytical characterization study in order to determine what chemical and/or physical differences resulted from the ageing process. FTIR-microscopy confirmed that the highest energy polymorph of CL-20 ( $\epsilon$ ) was prevalent in all 3 RSI-007 samples, so conversion of the

CL-20 to lower energy polymorphs during ageing is not the cause of the degraded performance. Although minor differences in binder additives were observed in the aged samples, the most significant difference in the aged samples was the decrease in included solvents (ethyl acetate and  $\text{CHCl}_3$ ) – likely resulting in increased sensitivity due to empty pores (i.e., hot spots) and crystal crazing similar to that previously observed for RDX [22]. In addition, since the solubility of CL-20 in ethyl acetate is extremely high, vaporization of the included solvent could have resulted in a loss of very small amounts of CL-20 from the composite energetic material, or perhaps the loss of the CL-20-saturated solvent inclusion resulted in an as yet unidentified change in initiation or reaction mechanism. Additional work to determine the validity of these hypotheses, including inclusion visualization with the aid of refractive index matching fluid [22], is on-going.

## Acknowledgements

Sandia National Laboratories is a multimission laboratory managed and operated by National Technology and Engineering Solutions of Sandia, LLC, a wholly owned subsidiary of Honeywell International, Inc., for the U.S. Department of Energy's National Nuclear Security Administration under contract DE-NA0003525.

## References

- [1] A. T. Nielsen, Caged polynitramine compound, US Patent Office, Patent No. US5693794A, Filing date 30 Sept 1988.
- [2] T. P. Russell, P. J. Miller, G. J. Piermarini, S. Block, Pressure/temperature phase diagram of hexanitrohexaazaisowurtzitane, *J. Phys. Chem.* **1993**, 97, 1993.
- [3] M. F. Foltz, C. L. Coon, F. Garcia, A. L. Nichols, The thermal stability of the polymorphs of hexanitrohexaazaisowurtzitane, Part I, *Propellants Explos. Pyrotech.* **1994**, 19, 19.
- [4] M. F. Foltz, C. L. Coon, F. Garcia, A. L. Nichols, The thermal stability of the polymorphs of hexanitrohexaazaisowurtzitane, Part II, *Propellants Explos. Pyrotech.* **1994**, 19, 133.
- [5] M. L. Chan, P. Carpenter, R. Hollins, M. Nadler, A. T. Nielsen, R. Nissan, D. J. Vanderah, R. Yee, R. D. Gilardi, *Chemical and physical properties of CL-20*. **1997**, Naval Research Laboratory. Report No. 1997–0559.
- [6] O. Bolton, L. R. Simke, P. F. Pagoria, A. J. Matzger, High Power Explosive with Good Sensitivity: A 2:1 Cocrystal of CL-20:HMX, *Cryst. Growth Des.* **2012**, 12, 4311.
- [7] J. L. Gottfried, Influence of exothermic chemical reactions on laser-induced shock waves, *Phys. Chem. Chem. Phys.* **2014**, 16, 21452.
- [8] J. L. Gottfried, Laboratory-scale method for estimating explosive performance from laser-induced shock waves, *Propellants Explos. Pyrotech.* **2015**, 40, 674.
- [9] S. A. Ramsden, P. Savic, A Radiative Detonation Model for the Development of a Laser-Induced Spark in Air, *Nature* **1964**, 203, 1217.
- [10] M. von Allmen, A. Blatter, *Laser-Beam Interactions with Materials: Physical Principles and Applications*, 2nd ed., Springer-Verlag, Berlin Heidelberg, **2002**.

- [11] J. L. Gottfried, Laser-induced plasma chemistry of the explosive RDX with various metallic nanoparticles, *Appl. Opt.* **2012**, *51*, B13.
- [12] D. Fischer, J. L. Gottfried, T. M. Klapötke, K. Karaghiosoff, J. Stierstorfer, T. G. Witkowski, Synthesis and Investigation of Advanced Energetic Materials Based on Bispyrazolymethanes, *Angew. Chem. Int. Ed.* **2016**, *128*, 16366.
- [13] J. L. Gottfried, T. M. Klapötke, T. G. Witkowski, Estimated detonation velocities for TKX-50, MAD-X1, BDNAPM, BTNPM, TKX-55 and DAAF using the laser-induced air shock from energetic materials technique, *Propellants Explos. Pyrotech.* **2017**, *42*, 353.
- [14] J. L. Gottfried, E. J. Bukowski, Laser-shocked energetic materials with metal additives: evaluation of chemistry and detonation performance, *Appl. Opt.* **2017**, *56*, B47.
- [15] E. S. Collins, J. L. Gottfried, Laser-induced deflagration for the characterization of energetic materials, *Propellants Explos. Pyrotech.* **2017**, *42*, 592.
- [16] J. L. Gottfried, F. C. De Lucia Jr, C. A. Munson, A. W. Miziolek, Laser-induced breakdown spectroscopy for detection of explosives residues: a review of recent advances, challenges, and future prospects, *Anal. Bioanal. Chem.* **2009**, *395*, 283.
- [17] J. L. Gottfried, Laser-induced air shock from energetic materials (LASEM) method for estimating detonation performance: challenges, successes and limitations, in: 20th Biennial APS Conference on Shock Compression of Condensed Matter, AIP Conf. Proc., St. Louis, MO, **2017**.
- [18] F. C. De Lucia Jr, J. L. Gottfried, Characterization of a series of nitrogen-rich molecules using laser-induced breakdown spectroscopy, *Propellants Explos. Pyrotech.* **2010**, *35*, 268.
- [19] X. Li, S. Chen, X. Wang, F. Shang, W. Dong, Z. Yu, Y. Yu, H. Zou, S. Jin, Y. Chen, Effect of polymer binders on safety and detonation properties of  $\epsilon$ -CL-20-based pressed-polymer-bonded explosives, *Mater. Express* **2017**, *7*, 209.
- [20] T. P. Russell, P. J. Miller, G. J. Piermarini, S. Block, High-pressure phase transition in gamma-hexanitrohexaazaisowurtzitane, *J. Phys. Chem.* **1992**, *96*, 5509.
- [21] S. Dumas, J. Y. Gauvrit, P. Lanteri, Determining the Polymorphic Purity of  $\epsilon$ -CL20 Contaminated by Other Polymorphs through the Use of FTIR Spectroscopy with PLS Regression, *Propellants Explos. Pyrotech.* **2012**, *37*, 230.
- [22] R. A. Pesce-Rodriguez, S. M. Piraino, *Characterization of Cyclohexanone Inclusions in Class 1 RDX*. **2014**, U.S. Army Research Laboratory: Aberdeen Proving Ground, MD. ARL-TR-6962.
- [23] J. J. Batten, The Thermal Decomposition of RDX below its Melting Point, *Australian J. Chem.* **1972**, *25*, 2337.
- [24] W. P. Bassett, B. P. Johnson, N. K. Neelakantan, K. S. Suslick, D. D. Dlott, Shock initiation of explosives: High temperature hot spots explained, *Appl. Phys. Lett.* **2017**, *111*, 061902.
- [25] A. van der Heijden, J. ter Horst, J. Kendrick, K. J. Kim, H. Kröber, F. Simon, U. Teipel, Crystallization, in: U. Teipel (Ed.) *Energetic Materials: Particle Processing and Characterization*, Wiley-VCH, **2005**, pp. 53.
- [26] R. J. Lieb, J. M. Heimerl, *Characteristics of JAX Gun Propellant*. **1994**, US Army Research Laboratory: Aberdeen Proving Ground, MD. ARL-TR-465.
- [27] V. Boddur, R. K. Toghiani, R. Damavarapu, *Solubility and Phase Behavior of CL20 in Supercritical Fluids*. **2006**, US Army Engineer Research and Development Center: Champaign, IL. ERDC/CERL TR-06-13.
- [28] R. A. Pesce-Rodriguez, E. Klier, *New micro-method for prediction of vapor pressure of energetic materials*. **2014**, US Army Research Laboratory: Aberdeen Proving Ground, MD. ARL-TR-6887.

Received: February 5, 2018

Revised: April 6, 2018

Published online: April 24, 2018